Sliding Mode Control of Underground Coal Gasification Process

Ali Arshad Uppal*, Vadim I. Utkin†, Yazan Alsmadi†, Aamer Iqbal Bhatti‡, and Shahid Ahmed Khan*,
* Department of Electrical Engineering, COMSATS Institute of Information Technology, Islamabad, Pakistan
† Electrical and Computer Engineering Department, The Ohio State University, Columbus, OH, USA
‡ Electrical and Electronic Engineering Department, Mohammad Ali Jinnah University, Islamabad, Pakistan

***Abstract*—The control of highly complex and nonlinear underground coal gasification (UCG) process is a challenging job. As the process occurs under the surface of the earth, so it is either impossible or very expensive to measure all the important parameters of the process, which further complicates the control design. The input of the UCG process is the flow rate of the injected air and the heating value of the product gas is the output. In this work a sliding mode control (SMC) algorithm is designed for a simplified model of an actual UCG process in order to maintain a desired constant heating value. The relative degree of the sliding variable is zero, because the input is readily available in it. As the heating value is the only measurement available, the trivial control design is not possible. Therefore, the time derivative of the control is selected as the system input, then the relative degree becomes one and the conventional SMC may be implemented. This approach let us maintain the output at the desired level and provides insensitivity with respect to different types of uncertainties. The stability of the zero dynamics is proved, which ensures that the overall system is stable. The simulation results demonstrate the robustness of the SMC design against the input disturbance and the modeling inaccuracies.**

***Index Terms*—Underground coal gasification (UCG) control, sliding mode control (SMC), relative degree and zero dynamics**

I. Introduction

COAL was first mined in Europe as early as 13th century, but it has been used as a source of energy for approximately 3 millenniums. During the industrial revolution in the 18th century it became an important source of energy. The biggest challenge for the coal industry was the environmental pollution caused by the combustion of coal, which produces oxides of sulphur and nitrogen. The detrimental impact of coal combustion on the environment was addressed by the advent of clean coal technologies which allow the removal of harmful gases before, during and after the burning of coal [1]. The gasification is one of the clean coal technologies in which coal is converted into a gas mixture. The high operating pressure of the gasification process assists the separation of the harmful gases [2]. Coal can either be gasified by extracting and purifying it on the surface or by the underground coal gasification (UCG) technology.

In UCG the coal is gasified underground. The oxidants (air and steam (H_2O (g)), or oxygen (O_2) and H_2O (g) or only air) are injected from one well which chemically react with coal to produce synthesis or syngas, which is collected from the other well. The synthesis gas (syngas) is a mixture of carbon monoxide (CO), hydrogen (H_2), methane (CH_4) and higher hydrocarbons (C_nH_m), which can be used in production of liquid fuels, industrial heating or as a fuel for power generation [3]–[5]. UCG is normally used for those coal fields which are either economically not feasible for mining or are not accessible by the conventional technology [1].

Corresponding author: V. I. Utkin (email: utkin.2@osu.edu).

The key indicators for the success of a UCG process are: calorific value of the syngas and the resource recovery of the coal seam [5], the later mostly depends on the configuration of the injection and production wells, where the former depends upon the type and geology of coal, effects of different physical and chemical phenomena occurring underground and operating conditions of the process. For a UCG site with specific coal type and well configuration, a constant and desired heating value of the syngas can be attained by optimizing the operating conditions. A mathematical model of the process is of paramount importance for determining the most suitable operating conditions. The research for the development of a mathematical model for a UCG process has been in progress since the early 20th century, which resulted in a number of mathematical models [6]–[15], but even the most complex three dimensional (3D) models do not perfectly describe the dynamics of the complex physicochemical process.

The control of UCG is an emerging area of research. In [16], [17] a lab scale UCG setup is controlled by some versions of the conventional PID controller [18]. However, the control of a field scale UCG process is a formidable job, especially considering the process nonlinearities and underground disturbances. Some other factors also make the control of the process a challenging job. The mass and heat transfer phenomena in UCG can be effectively modeled by partial differential equations (PDEs) with at least two independent variables, one each for time and length, and control of such systems is not a trivial task [19], [20]. Another factor which increases difficulty in control design is the unavailability of the measurement of important model parameters. As the process of UCG takes place underground, and it is either impossible or very expensive and difficult to install sensors at different locations in the reactor, so normally the available measurement is molar fraction of the product gases recovered at the production well. Therefore, for UCG system with nonlinearities, underground disturbances and uncertainties a control technique is required which can keep a constant desired heating value of syngas, in spite of fact that design procedure is performed based on approximate model. One such technique is the sliding mode

control (SMC) [21], [22]. In [23] and [24] a first and second order SMC algorithms are implemented on two different UCG process models to maintain a constant heating value at the production well respectively. The time domain mathematical model in [23] is a very crude representation of the actual UCG process, as it assumed that the input, output and all the chemical reactions occur at the same location along the length of the reactor. The work in [24] uses a validated model of actual UCG process [25], but during the control design it is assumed that the total concentration of all the gases stays constant through out the length of the reactor, which is not true.

The contribution of this paper is twofold: development of a control oriented model by incorporating certain assumptions in the model of [25], and design of SMC for the model. The model simplifications help in the analytical design of the controller. The SMC algorithm is designed for the model to control the heating value of the product gases. The design idea of SMC implies two steps:

1) Selecting switching surface such that sliding mode along this surface, governed by reduced order equation exhibits the desired properties.
2) The control input should enforce sliding mode.

In the paper such surface is selected and then discontinuous control is designed, such that for any initial condition the state reaches the surface after finite time interval and then sliding mode appears with desired dynamics. The designed control solves the main problem to maintain the variable under control at desired level. However, the system is acceptable only if overall motion in sliding mode is stable. In literature this dynamics is called internal or zero dynamics [26]. It is shown in the paper that zero dynamics for the process under control are stable. The above results were obtained for the simplified model. As the simulation results show, the control demonstrates the same properties being applied to the actual model of the process.

The rest of the article is arranged as follows: The components of the UCG control system are explained in Section II, the simplifications introduced for the model based control of the process are discussed in Section III, the problem statement is presented in Section IV, the control procedure is outlined in Section V, the steps involved in the design of SMC are demonstrated in Section VI, numerical solution of the closed loop system is detailed in Section VII, Section VIII discusses the simulations results and the article is concluded in Section IX.

II. Components of the UCG control system

The block diagram in Fig. 1 shows the components of UCG control system. The controller computes the flowrate of the air: u (moles/cm^2/s) based on the measured (y_m) and desired (y_r) heating values (KJ/m^3) of the product gases coming out of the UCG system. The heating value y is computed by the gas analyzer after measuring the composition of the product gases recovered from the production well. The procedure for calculating y is given in Appendix B. The flow rate of the steam δ acts as an input disturbance for the system. The value of δ is unknown but it needs to be in a certain range for the process to be operational [24], [25], [27]. The control valve and gas analyzer are modeled with first order transfer functions with time delays, which are given in Eqs. (1) and (2) respectively.

$$G_1(s) = \frac{\exp\left(-\tau_{d_a} s\right)}{\tau_a s + 1} \tag{1}$$

$$G_2(s) = \frac{\exp\left(-\tau_{d_g} s\right)}{\tau_g s + 1} \tag{2}$$

where τ_a and τ_g are the time constants (s) for the control valve and gas analyzer systems respectively, τ_{d_a} and τ_{d_g} represent the input and output delays of the system and y is the heating value of the product gases.

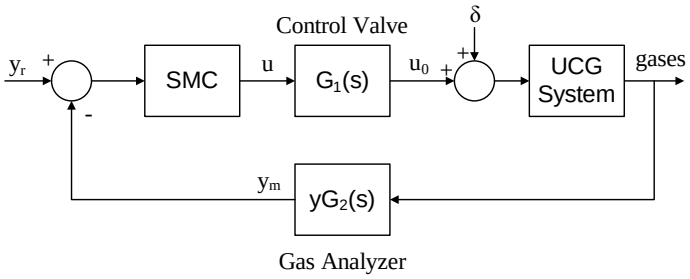

Fig. 1. Block diagram of UCG control system

A. UCG system

The reactor model of UCG consists of coal, char and eight gases: CO, carbon dioxide (CO_2), H_2, H_2O (g), CH_4, nitrogen (N_2), O_2 and tar. The tar is used to close the stoichiometry of coal pyrolysis reaction [8], and the traces of higher hydrocarbons (C_nH_m) produced are also included in it. The schematic of the UCG process is shown in Fig. 2. Air at particular flowrate u_0 enters the UCG reactor from the injection well ($x = 0$), while the product gases produced as the result of various oxidation and gasification reactions are recovered from the production well ($x = L$).

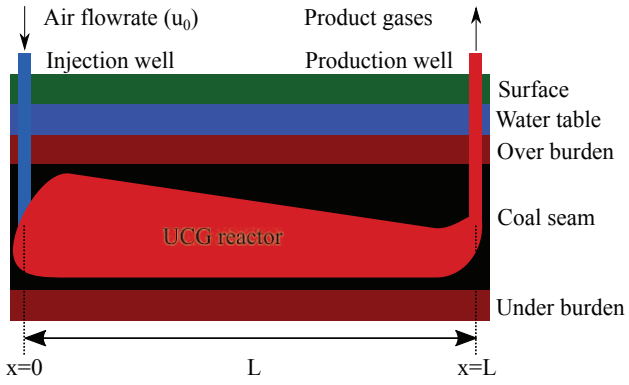

Fig. 2. Schematic of UCG process

III. Simplifications considered for the model based control

In order to simplify the control design the dynamics of control valve and gas analyzer are ignored, which implies $u_0 = u$ and $y = y_m$. Some simplifications are also made in the actual mathematical model of the UCG reactor.

A. Control oriented model of UCG

The complete model and assumptions considered for its simplification are detailed in Appendix A. The following PDEs represent the states of the UCG system:

$$\frac{\partial \rho_1}{\partial t} = -M_1 R_1 \tag{3}$$
$$\rho_1(0,x) = \rho_{1_0}(x), \quad 0 \le x \le L$$
$$\frac{\partial \rho_2}{\partial t} = M_2\left[|a_{s_{2,1}}|R_1 - R_2(u) - R_3(u)\right] \tag{4}$$
$$\rho_2(0,x) = \rho_{2_0}(x), \quad 0 \le x \le L$$
$$\frac{\partial T_s}{\partial t} = \frac{B\frac{\partial^2 T_s}{\partial x^2} + h(T - T_s) - q_1 R_1 - q_2 R_2(u) - q_3 R_3(u)}{(cp_1\rho_1 + cp_2\rho_2)} \tag{5}$$
$$T_s(0,x) = T_{s_0}(x), \quad 0 \le x \le L$$
$$\frac{\partial T_s}{\partial x}(t,0) = \frac{\partial T_s}{\partial x}(t,L) = 0, \quad t \ge 0$$
$$where,$$
$$R_1 = 5\frac{\rho_1}{M_1}\exp\left(\frac{-6039}{T_s}\right) \tag{6}$$
$$R_2 = \frac{v_g C_7}{u+\delta} CR_2 \tag{7}$$
$$C_7 = 0.21\frac{u}{v_g}\exp\left(-\frac{|a_{7,2}|}{u+\delta}\int_0^x CR_2 dx\right)$$
$$CR_2 = \frac{9.55\times 10^8 \rho_2 P \exp\left(\frac{-22142}{T_s}\right) k_y}{M_2 k_y\sqrt{T_s} + 9.55\times 10^8 \rho_2 P \exp\left(\frac{-22142}{T_s}\right)}$$
$$R_3 = \frac{\delta}{\delta+u} CR_3 \tag{8}$$
$$CR_3 = \frac{k_y P^2 \rho_2 E_1}{P^2 E_1 \rho_2 + k_y M_2 (P+E_2)^2}$$
$$E_1 = \exp\left(5.052 - \frac{12908}{T_s}\right)$$
$$E_2 = \exp\left(-22.216 + \frac{24880}{T_s}\right)$$

where $\rho_1(t,x)$ and $\rho_2(t,x)$ are densities of coal and char (g/cm^3), M_1 and M_2 are molecular weights of coal and char (g/mol), t and x are variables for time (s) and length (cm), $L = 2500cm$ is the length of the reactor, $a_{s_{2,1}}$ is the stoichiometric coefficient of char in coal pyrolysis reaction, $T_s(t,x)$ and T are solid and gas temperatures (K), h is the heat transfer coefficient (cal/s/K/cm^3), q_i is the heat of reaction i (cal/mol), B is a constant depending on the coal bed porosity and thermal conductivity of coal and char (cal/cm/s/K), v_g is the superficial velocity of gases (cm/s), c_{p_1} and c_{p_2} are the heat capacities for coal and char respectively (cal/g/K), $R_i(\rho_1, \rho_2, T_s, u)$ is rate of the chemical reaction i, with $i = 1,2,3$ represents pyrolysis, char oxidation and steam gasification respectively, $a_{i,j}$ is the stoichiometric coefficient of gas i in reaction j and H_i is the heat of combustion (KJ/m^3) of gas i with $i = 1,3,5,8$ represents CO, H_2, CH_4 and tar respectively, C_7 is the distribution of O_2 concentration (mol/cm^3) along x, $a_{7,2}$ is the stoichiometric coefficient of O_2 in char oxidation reaction, P is the pressure of gases (atm) and k_y is the mass transfer coefficient (mol/cm^3/s).

The concentration of the gases at the production well are given by Eqs. (49) and (50). As the dynamics of the gas analyzer are ignored, therefore, $y = y_m$ is given by Eq. (9)

$$y = \frac{100\left(\alpha\int_0^L R_1 dx + \beta\int_0^L R_3 dx\right)}{\gamma\int_0^L R_1 dx + \eta\int_0^L R_3 dx + \zeta\int_0^L R_2 dx + 0.79\frac{u}{v_g}} \tag{9}$$
$$\alpha = \frac{1}{v_g}(a_{11}H_1 + a_{31}H_3 + a_{51}H_5 + a_{81}H_8)$$
$$\beta = \frac{1}{v_g}(a_{13}H_1 + a_{33}H_3)$$
$$\gamma = \frac{1}{v_g}(a_{11} + a_{21} + a_{31} + a_{51} + a_{81})$$
$$\eta = \frac{1}{v_g}(a_{13} + a_{33})$$
$$\zeta = \frac{a_{2,2}}{v_g}$$

The complete derivation of Eq. (9) is given in Appendix. B.

IV. Problem statement

The objective of the research is to design the control for the UCG process, which maintains the heating value at the desired level. The control problem should be solved in the presence of modeling inaccuracies and external disturbance. Therefore, the control problem can be rephrased as to make $y = y_r$, in the presence of external disturbance δ and modeling inaccuracies. Due to the fact that y is the only measurement available [24], [25], the job of the control system design becomes even more challenging.

V. Outline of the design procedure

1) The sliding variable s is selected, such that sliding mode has desired properties. In arbitrary finite dimensional system with state $x \in \Re^n$, sliding mode appears if values $s(x)$ and $\dot{s}(x)$ have different signs. It means $\dot{s}(x)$ should depend on discontinuous control.
2) Discontinuous control is selected to enforce sliding mode based on the above condition: $s(x)$ and $\dot{s}(x)$ should have different signs.
3) Analysis of zero dynamics.

VI. Control design

A. Selection of sliding variable

The sliding variable is selected in order to keep the heating value at a desired constant level.

$$s = y_r - y \tag{10}$$

In order to meet the desired objective we need $s = 0 \implies y = y_r$, and then control can be designed by substituting Eq. (9) in Eq. (10).

$$\frac{100\left[\alpha\int_0^L R_1dx + \beta\int_0^L R_3dx\right]}{\gamma\int_0^L R_1dx + \eta\int_0^L R_3dx + \zeta\int_0^L R_2dx + 0.79\frac{u}{v_g}} = y_r \tag{11}$$

$$\sigma_1 + \sigma_2\frac{\delta}{u+\delta} - \sigma_3\frac{u}{u+\delta} - \sigma_4 u = 0$$

$$u^2\sigma_4 + u\left(-\sigma_1 + \sigma_3 + \delta\sigma_4\right) - \delta\left(\sigma_1 + \sigma_2\right) = 0$$

$$u_1 = \frac{-b + \sqrt{b^2 - 4ac}}{2a}$$

$$u_2 = \frac{-b - \sqrt{b^2 - 4ac}}{2a}$$

$where,$

$$a = \sigma_4$$

$$b = -\sigma_1 + \sigma_3 + \delta\sigma_4$$

$$c = -\delta\left(\sigma_1 + \sigma_2\right)$$

$$\sigma_1 = \left(100\alpha - \gamma y_r\right)\int_0^L R_1dx$$

$$\sigma_2 = \left(100\beta - \eta y_r\right)\int_0^L CR_3dx$$

$$\sigma_3 = 0.21\zeta y_r\int_0^L CR_2dx$$

$$\sigma_4 = 0.79\frac{y_r}{v_g}$$

where u_1 and u_2 are real as $\left(b^2 - 4ac\right) > 0$, also $\sqrt{b^2 - 4ac} > b$ & $a > 0\ \forall t$, and only valid solution is u_1, because the molar flow rate of the air can not be negative.

However, the trivial control design is not realizable, because the right hand side of u_1 contains state variables and miscellaneous process parameters which are not measurable. So we try to overcome this problem by enforcing sliding mode and inserting integrator in the input, such that $\dot{u} = \nu$ and $\nu = -\kappa\,\mathrm{sign}\left(s\right),\ \kappa \in R^+$. Therefore, $\dot{s}$ depends on discontinuous control ν and necessary control can be found using sliding mode as shown in Fig. 3. Moreover, this approach does not need the information about system's states. Further, sliding mode can be enforced with $y = y_r$ by a proper choice of gain κ.

It is required to find derivative of the sliding variable in the form $\dot{s} = \nu\phi + \theta$, where ϕ and θ are state functions.

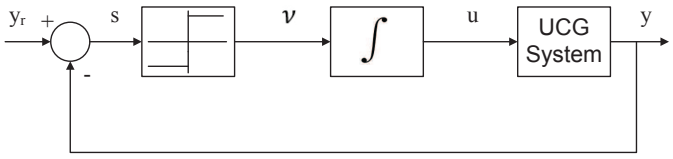

Fig. 3. SMC design for UCG system

$$\dot{s} = \dot{y_r} - \dot{y} \tag{12}$$

$$\dot{y} = \frac{100}{D^2}\left(D\dot{N} - N\dot{D}\right)$$

$where,$

$$N = \alpha\int_0^L R_1dx + \beta\int_0^L R_3dx$$

$$D = \gamma\int_0^L R_1dx + \eta\int_0^L R_3dx + \zeta\int_0^L R_2dx + \frac{0.79}{v_g}u$$

$$\dot{N} = \alpha\int_0^L \dot{R_1}dx + \beta\int_0^L \dot{R_3}dx$$

$$\dot{D} = \gamma\int_0^L \dot{R_1}dx + \eta\int_0^L \dot{R_3}dx + \zeta\int_0^L \dot{R_2}dx + \frac{0.79}{v_g}\dot{u}$$

$where,$

$$\dot{R_3} = \left(\frac{\delta}{u+\delta}\right)C\dot{R_3} + CR_3\frac{d}{dt}\left(\frac{\delta}{u+\delta}\right)$$

$$= \left(\frac{\delta}{u+\delta}\right)C\dot{R_3} + \frac{CR_3}{\left(u+\delta\right)^2}\left(u\dot{\delta} - \delta\dot{u}\right)$$

$$\dot{R_2} = 0.21\frac{d}{dt}\left(\frac{uCR_2E_u}{u+\delta}\right)$$

$$= \dot{u}\omega + \psi$$

$where,$

$$E_u = \exp\left(-\frac{|a_{7,2}|}{u+\delta}\int_0^L CR_2dx\right)$$

$$\omega = \frac{|a_{7,2}|uCR_2E_u\int_0^L CR_2dx}{4.762\left(u+\delta\right)^3} + \frac{\delta E_u\int_0^L CR_2dx}{4.762\left(u+\delta\right)^2}$$

$$\psi = \frac{uE_u\dot{\delta}CR_2\int_0^L CR_2dx}{4.701\left(u+\delta\right)^3} - \frac{uE_u\dot{\delta}CR_2}{4.762\left(u+\delta\right)^2} + \frac{uE_uC\dot{R_2}}{4.762\left(u+\delta\right)}$$

By substituting $\dot{y_r} = 0$ (y_r is constant) and $\dot{y}$ in Eq. (12), the closed form expression for $\dot{s}$ takes the desired form

$$\dot{s} = \nu\phi + \theta,\ \dot{u} = \nu \tag{13}$$

$where,$

$$\phi = 100\frac{N\varphi}{D^2}$$

$$\theta = \frac{100}{D^2}\left[N\left(\vartheta_1 + \vartheta_2\right) - D\vartheta_3\right]$$

$$
\begin{aligned}
&where,\\
&\varphi = \frac{0.79}{v_g} + \frac{\int_0^L CR_3 dx}{(u+\delta)^2}(\beta-\delta) + \zeta\int_0^L \omega dx\\
&\vartheta_1 = \int_0^L \dot{R}_1 dx\,(\gamma-\alpha) + \zeta\int_0^L \psi dx\\
&\vartheta_2 = \frac{\eta}{(u+\delta)}\left[\frac{u\dot{\delta}\int_0^L CR_3 dx}{(u+\delta)} + \delta\int_0^L C\dot{R}_3 dx\right]\\
&\vartheta_3 = \frac{\beta}{(u+\delta)}\left[\frac{u\dot{\delta}\int_0^L CR_3 dx}{(u+\delta)} + \delta\int_0^L C\dot{R}_3 dx\right]
\end{aligned}
$$

The function $\phi = 100\frac{N\varphi}{D^2} > 0, \forall t \geq 0$, because N, D and φ in Eqs. (12) and (13) depend upon R_1, R_2, R_3, u, δ and v_g which are always positive. Moreover, the constants α, β, γ, η and ζ in Eq. (9) are also positive and $\beta >> \delta$ in φ. The function $\phi(t)$ is bounded by Φ_l and Φ_u such that: $0 < \Phi_l \leq \phi(t) \leq \Phi_u$, and $\theta(t)$ is upper bounded by Θ_u: $\|\theta(t)\| \leq \Theta_u$.

As $\phi(t) > 0, \forall t \geq 0$, therefore sliding mode can be enforced by selecting a suitable value of discontinuous controller gain κ.

B. Enforcing sliding mode

In order to prove the existence of sliding mode a positive definite Lyapunov function is chosen and its time derivative is found.

$$
\begin{aligned}
V &= \frac{1}{2}s^2 \qquad (14)\\
\dot{V} &= s\dot{s}\\
&= s\,(\nu\phi + \theta)\\
&= s\,(-\kappa\,\mathrm{sign}\,(s)\phi + \theta)\\
&\leq |s|\,(-\kappa\Phi_l + \Theta_u)
\end{aligned}
$$

If $\kappa = \frac{\tau + \Theta_u}{\Phi_l}$ with $\tau \in R^+$, then the derivative of the Lyapunov function is negative definite, and sliding mode exists.

$$\dot{V} \leq -\tau|s| \qquad (15)$$

Even more, sliding mode occurs after a finite time interval [28], and the main control problem is solvable.

C. Stability of the zero dynamics

The relative degree r of sliding variable s is zero, because u is readily available in s. Therefore, all the state equations in Section III-A constitute the zero dynamics of the system with $u = u_1$ (Eq. (11)), which makes $s = 0$ [26]. After the establishment of sliding mode it is mandatory to check whether the motion of the system called zero dynamics is stable.

The zero dynamics are comprised of following set of equations, after $t \geq t_{ss}$ when $s = 0$. The Eqs. (16), (17) and (18) are obtained by replacing $R_i(\rho_1, \rho_2, T_s, u)$ by $\tilde{R}_i\left(\tilde{\rho_1}, \tilde{\rho_2}, \tilde{T_s}, u_1\right)$ in Eqs. (3), (4) and (5).

$$
\begin{aligned}
\frac{\partial\tilde{\rho_1}}{\partial\tilde{t}} &= -M_1\tilde{R}_1 \qquad (16)\\
\frac{\partial\tilde{\rho_2}}{\partial\tilde{t}} &= M_2\left(|a_{s_{2,1}}|\tilde{R}_1 - \tilde{R}_2 - \tilde{R}_3\right) \qquad (17)\\
\frac{\partial\tilde{T_s}}{\partial\tilde{t}} &= \frac{1}{C_s}\left[B\frac{\partial^2\tilde{T_s}}{\partial x^2} + h(T-\tilde{T_s}) - H_s\right] \qquad (18)\\
&where,\\
&C_s = cp_1\tilde{\rho_1} + cp_2\tilde{\rho_2}\\
&H_s = -|q_1|\tilde{R}_1 - |q_2|\tilde{R}_2 + |q_3|\tilde{R}_3
\end{aligned}
$$

where $\tilde{t} = t - t_{ss}$ and H_s is the heat source generated from the chemical reactions. Since coal pyrolysis and char oxidation reactions are exothermic in nature, hence there heat of reaction is negative [25].

The boundedness of the zero dynamics is investigated in the subsequent paragraphs.

The solution of Eq. (16) is given as:

$$
\begin{aligned}
&\tilde{\rho_1}\left(\tilde{t}, x\right) = C\exp\left(-5E_3\tilde{t}\right) \qquad (19)\\
&where,\\
&C(x) = \tilde{\rho_1}(0, x)\\
&E_3(x) \leq \exp\left\{\frac{-6039}{\max\limits_{\tilde{t}\geq 0}\tilde{T_s}\left(\tilde{t}, x\right)}\right\}
\end{aligned}
$$

It is important to note that for $0 < \tilde{T}_{smin} \leq \tilde{T_s}(\tilde{t}, x) \leq \infty$, the distribution $\tilde{\rho_1}(0, x)$ exponentially decays with time.

In order to evaluate the boundedness of $\tilde{\rho_2}$ and $\tilde{T_s}$, it is important to show that $\tilde{R}_1$, $\tilde{R}_2$, $\tilde{R}_3$ and u_1 are bounded. The Eqs. (6), (7) and (8) show that the reaction rates are dependent on $\tilde{\rho_1}$, $\tilde{\rho_2}$ and $\tilde{T_s}$. It has been proved in Eq. (19) that $\tilde{\rho_1}$ is stable, which also implies the stability of $\tilde{\rho_2}$, because $\tilde{\rho_1}$ is decomposed by coal pyrolysis reaction to yield $\tilde{\rho_2}$ and product gases, therefore, for law of conservation of mass to hold:

$$\max_{\substack{0\leq x\leq L\\ \tilde{t}\geq 0}} \tilde{\rho_2}(\tilde{t}, x) < \max_{\substack{0\leq x\leq L\\ \tilde{t}\geq 0}} \tilde{\rho_1}(\tilde{t}, x)$$

Now it can be inferred from Eqs. (6), (7) and (8) that for any $\tilde{T_s}$: $0 < \tilde{T}_{smin} \leq \tilde{T_s}(\tilde{t}, x) \leq \infty$, the reaction rates are bounded. The input u_1 is also bounded as it is the function of the reaction rates (Eq. (11)).

Th complete solution of Eq. (17) is found by rewriting it in the following form, which is obtained by substituting Eqs. (7) and (8) in Eq. (17).

$$\frac{\partial\tilde{\rho_2}}{\partial\tilde{t}}+\tilde{\rho_2}\xi=\chi \tag{20}$$
$$where,$$
$$\chi(x)\leq|a_{s_{2,1}}|M_2\tilde{R_1}\big|_{\max\limits_{\tilde{t}\geq0}T_s(\tilde{t},x)}$$
$$\xi(x)\leq\left(\frac{0.21u_1\tilde{E_u}\Pi_1}{\delta+u_1}+\frac{\delta\Pi_2}{\delta+u_1}\right)\Bigg|_{\max\limits_{\tilde{t}\geq0}T_s(\tilde{t},x),U_1,\Delta}$$
$$\Pi_1=\frac{9.55\times10^8P\exp\left(\frac{-22142}{\tilde{T_s}}\right)k_y}{M_2k_y\sqrt{\tilde{T_s}}+9.55\times10^8\rho_2P\exp\left(\frac{-22142}{\tilde{T_s}}\right)}$$
$$\Pi_2=\frac{k_yP^2\tilde{E_1}}{P^2\tilde{E_1}\rho_2+k_yM_2\left(P+\tilde{E_2}\right)^2}$$
$$\tilde{E_u}=\exp\left(-\frac{|a_{7,2}|}{u_1+\delta}\int_0^x C\tilde{R}_2dx\right)$$

where $0<u_1\leq U_1$, $0<\delta\leq\Delta$, $\tilde{E_1}=E_1(\tilde{T_s})$, $\tilde{E_2}=E_2(\tilde{T_s})$ and $C\tilde{R}_2=CR_2(\tilde{T_s})$. The parameters CR_2, E_1 and E_2 are given in Eqs. (7) and (8).

Now (20) can be solved as a linear PDE.

$$Let,\ \varpi\left(\tilde{t}\right)=\exp\left(\int\xi d\tilde{t}\right)$$
$$\frac{\partial\tilde{\rho_2}}{\partial\tilde{t}}\varpi\left(\tilde{t}\right)+\varpi\left(\tilde{t}\right)\tilde{\rho_2}\xi=\chi\varpi\left(\tilde{t}\right)$$
$$\int\frac{d}{d\tilde{t}}\left[\tilde{\rho_2}\exp\left(\xi\tilde{t}\right)\right]d\tilde{t}=\chi\int\exp\left(\xi\tilde{t}\right)d\tilde{t}$$
$$\tilde{\rho_2}\left(\tilde{t},x\right)=\underbrace{\frac{\chi\left(\tilde{t},x\right)}{\xi\left(\tilde{t},x\right)}}_{S_1}+\underbrace{C\exp\left[-\xi\left(\tilde{t},x\right)\tilde{t}\right]}_{S_2} \tag{21}$$
$$where,$$
$$C\left(x\right)=\left[\tilde{\rho_2}\left(0,x\right)-\frac{\chi\left(0,x\right)}{\xi\left(0,x\right)}\right]$$

Before investigating the solution of $\tilde{\rho_2}(\tilde{t},x)$ in (21), a brief description of the reaction zone [25] within the UCG reactor is mandatory. The reaction zone Ω is a region along the length of the reactor, where all the chemical reactions occur, when $\tilde{\rho_1},\tilde{\rho_2}>0$ then: $x=0<x_r\leq\Omega\leq x_p<x=L$. The boundary of Ω towards $x=L$ is x_p which represents the *pyrolysis front*, whereas x_r towards $x=0$ corresponds to the *reaction front*. The pyrolysis reaction occurs in the proximity of x_p with rate $\tilde{R_1}$, yielding char and product gases. The char produced by pyrolysis reaction spans whole Ω. The region beyond x_p contains unreacted coal, while the region before x_r contains ash produced from the burnt coal and char. The values of $\tilde{R_2}$ and $\tilde{R_3}$ are only significant near x_r, because $\tilde{T_s}$ has its maximum value here.

Now it can be inferred from (21) that $\tilde{\rho_2}$ is produced near x_p with rate determined by S_1. The $\tilde{\rho_2}$ is consumed by $\tilde{R_2}$ and $\tilde{R_3}$ near x_r as suggested by S_2. The reaction zone Ω moves towards $x=L$ with time, as the coal and char are continuously consumed by the reactants: O_2 and H_2O (g). Therefore, when all the coal is consumed in the reactor then production of $\tilde{\rho_2}$ is ceased and it is only consumed around x_r:

$$\tilde{\rho_2}\left(\tilde{t},x\right)=\left[\rho_2\left(0,x\right)-\frac{\chi\left(0,x\right)}{\xi\left(0,x\right)}\right]\exp\left(-\xi\tilde{t}\right)$$

The heat equation in (18) can be rewritten as:

$$C_s\dot{\tilde{T_s}}=B\tilde{T_s}''-h\tilde{T_s}+hT(x)+H_s \tag{22}$$
$$with,$$
$$\tilde{T_s}(0,x)=\tilde{T_{s_0}}(x)$$
$$\tilde{T_s}'(\tilde{t},0)=\tilde{T_s}'(\tilde{t},L)=0$$

where $\dot{\tilde{T}}_s=\frac{\partial\tilde{T_s}}{\partial\tilde{t}}$, $\tilde{T_s}'=\frac{\partial\tilde{T_s}}{\partial x}$ and $\tilde{T_s}''=\frac{\partial^2\tilde{T_s}}{\partial x^2}$.

The solution of Eq. (22) is acceptable if it is not unstable, strictly speaking we need to show that the solution is bounded. Formally speaking we have to deal with the analysis of a complex nonlinear system, since H_s depends on $\tilde{T_s}$. But as it has been shown previously that all the reaction rates are bounded for any value of $\tilde{T_s}$, hence H_s is also bounded. Therefore, our problem may be reformulated in the following way. It should be shown that solution to the linear PDE:

$$\dot{\tilde{T}}_s=\frac{1}{C_s}\left[B\tilde{T_s}''-h\tilde{T_s}+hT(x)+\mathcal{G}(\tilde{t},x)\right] \tag{23}$$
$$where,$$
$$|\mathcal{G}(\tilde{t},x)|\leq\mathcal{G}_0,\ \mathcal{G}_0\in\Re^+$$

can be represented in the following form:

$$\tilde{T_s}=\Delta\tilde{T_s}+\tilde{T}_{sx}+\tilde{T}_{sd} \tag{24}$$

where $\Delta\tilde{T_s}$ corresponds to the solution without the inputs $T(x)$ and $\mathcal{G}$, $\tilde{T}_{sx}$ is the forced component defined by $T(x)$ and $\tilde{T}_{sd}$ is the forced part which depends on the disturbance $\mathcal{G}(\tilde{t},x)$.

The boundedness of all the solution components in Eq. (24) is investigated independently.

Consider the homogeneous heat equation:

$$C_s\Delta\dot{\tilde{T}}_s=B\Delta\tilde{T_s}''-h\Delta T_s \tag{25}$$
$$with,$$
$$\Delta\tilde{T_s}(0,x)=\Delta\tilde{T_{s_0}}(x)$$
$$\Delta\tilde{T_s}'(\tilde{t},0)=\Delta\tilde{T_s}'(\tilde{t},L)=0$$

The stability of Eq. (25) is investigated by the Lyapunov functional:

$$V=\frac{1}{2}\int_0^L C_s\Delta\tilde{T_s}^2dx \tag{26}$$

The time derivative of V is given as:

$$\dot{V} = \underbrace{\int_0^L \Delta\tilde{T}_s C_s \Delta\dot{\tilde{T}}_s dx}_{\dot{V}_1} + \underbrace{\frac{1}{2}\int_0^L \Delta\tilde{T}_s{}^2 \dot{C}_s dx}_{\dot{V}_2} \tag{27}$$

$where,$

$$\begin{aligned}
\dot{V}_1 &= B\int_0^L \Delta\tilde{T}_s \left(\Delta\tilde{T}_s{}'\right)' dx - h\int_0^L \Delta\tilde{T}_s{}^2 dx \\
&= -B\int_0^L \left(\Delta\tilde{T}_s{}'\right)^2 dx - h\int_0^L \Delta\tilde{T}_s{}^2 dx \\
\dot{V}_2 &= \frac{1}{2}\int_0^L \Delta\tilde{T}_s{}^2 \left(cp_1\dot{\tilde{\rho}}_1 + cp_2\dot{\tilde{\rho}}_2\right) dx \\
&= -\frac{\left(M_1 cp_1 - |a_{s_{2,1}}| cp_2 M_2\right)}{2}\int_0^L \tilde{R}_1 \Delta\tilde{T}_s{}^2 dx \\
&\quad - \frac{M_2 cp_2}{2}\int_0^L \Delta\tilde{T}_s{}^2 \left(\tilde{R}_2 + \tilde{R}_3\right) dx
\end{aligned}$$

where $M_1 cp_1 > |a_{s_{2,1}}| cp_2 M_2$.

As the derivative of the Lyapunov functional in Eq. (27) is strictly negative, hence $\Delta\tilde{T}_s$ is asymptotically stable.

The following boundary value problem is solved to yield $\tilde{T}_{sx}$

$$\begin{aligned}
&B\tilde{T}_{sx}'' - h\tilde{T}_{sx} + hT(x) = 0 \\
&\tilde{T}_{sx}'(t,0) = \tilde{T}_{sx}'(t,L) = 0
\end{aligned} \tag{28}$$

The gas temperature $T(x)$ is obtained by solving the linear ODE in Eq. (42)

$$T(x) = T(0)\exp(-\lambda x) + \lambda\int_0^x \exp\{-\lambda(x-\mathcal{X})\}\tilde{T}_s(\mathcal{X})d\mathcal{X} \tag{29}$$

where $\lambda = \dfrac{h}{v_g C_g}$ is a constant

Eq. (28) can be rewritten in the following form by substituting $h(T - \tilde{T}_s) = -v_g C_g T'$ from Eq. (42)

$$B\tilde{T}_{sx}'' - v_g C_g T' = 0 \tag{30}$$

By differentiating Eq. (29) with respect to x and substituting T' in Eq. (30) yields the nonhomogeneous boundary value problem:

$$B\tilde{T}_{sx}'' - h\tilde{T}_{sx} = -\Lambda\exp(-\lambda x) \tag{31}$$

where $\Lambda = h\left[T(0) + \tilde{T}_s(0,0)\right]$ is a constant

The overall solution of Eq. (31) is: $\tilde{T}_{sx} = \tilde{T}_{sc} + \tilde{T}_{sp}$. The complementary solution $\tilde{T}_{sc}$ is obtained by solving the following equation:

$$B\tilde{T}_{sx}'' - h\tilde{T}_{sx} = 0 \tag{32}$$

The characteristic polynomial for the second order ODE is: $r^2 - \dfrac{h}{B} = 0$, which yields $r = \pm\sqrt{\dfrac{h}{B}}$. The general form of $\tilde{T}_{sc}$ is given as:

$$\tilde{T}_{sc} = C_1\exp\left(\sqrt{\frac{h}{B}}\right) + C_2\exp\left(-\sqrt{\frac{h}{B}}\right) \tag{33}$$

After incorporating the boundary conditions, $\tilde{T}_{sc} = 0$, as $C_1 = C_2 = 0$.

Let the particular solution be: $\tilde{T}_{sp} = \mathcal{A}\exp(-\lambda x)$. Now by substituting $\tilde{T}_{sp}$ in Eq.(31) the value of constant $\mathcal{A}$ is obtained

$$\begin{aligned}
&B\mathcal{A}\lambda^2\exp(-\lambda x) - h\mathcal{A}\exp(-\lambda x) = -\Lambda\exp(-\lambda x) \\
&\mathcal{A} = -\frac{\Lambda}{\lambda^2 B - h}
\end{aligned} \tag{34}$$

The solution $\tilde{T}_{sx}$ is given as:

$$\tilde{T}_{sx} = -\frac{\Lambda}{\lambda^2 B - h}\exp(-\lambda x) \tag{35}$$

Therefore, the forced response $\tilde{T}_{sx}$ due to $T(x)$ is also bounded.

As the disturbance $\mathcal{G}$ in Eq. (22) is bounded, therefore, $\tilde{T}_{sd}$ is also bounded. The boundedness of $\tilde{T}_{sd}$ can be shown if it is represented in the modal form [29]. All the solution components of Eq. (24) are bounded, therefore, $\tilde{T}_s$ stays bounded throughout the process of gasification.

The results in (19), (21) and boundedness of $\tilde{T}_s$ show that the zero dynamics of the UCG process are bounded and SMC design is valid.

VII. Numerical solution of the closed loop system

In order to asses the robustness of SMC against modeling inaccuracies and input disturbance, the dynamics of control valve and gas analyzer, and the actual UCG reactor model given in [25] is used in the simulations. The UCG control system in Fig. 1 is solved in Matlab. The time delays associated with control valve and gas analyzer are replaced with first order Pade approximation [30]. For a time delay of τ_d s the first order Pade approximation for $\exp(-\tau_d s)$ is given by:

$$\exp(-\tau_d s) \approx \frac{-\tau_d s + 2}{\tau_d s + 2}$$

The UCG reactor model is solved in two modes: ignition for first t_0 s and then gasification for $t > t_0$. The purpose of the ignition is to heat up the coal seam so that it becomes conducive to the gasification reactions. During the ignition phase the only reaction taking place in the UCG reactor is that of the coal pyrolysis, the gasification reactions do not occur in this phase due to the absence of steam. The detail description of the solution of the UCG reactor can be found in [24], [25], but, in order to keep the interest of the reader a brief description of the solution strategy is given in Table I.

TABLE I
SOLUTION OF THE UCG REACTOR MODEL

1. Input all the model parameters
2. Initialize the solid subsystem (Eqs. (3), (4) and (5)): $\rho_i(0,x) = \rho_{i_0}(x)$ and $T_s(0,x) = T_{s_0}(x)$
3. Solve gas Eqs. (41), (42), (43) and (44) to yield there initial distributions with following inlet boundary conditions: $C_i(0) = \left[0\ 0\ 0\ 0\ 0\ \frac{0.79u_{0_{ol}}}{v_{g_0}}\ \frac{0.21u_{0_{ol}}}{v_{g_0}}\ 0\right]$, $T(0) = T_0$, $v_g(0) = v_{g_0}$ and $P(0) = P_0$
4. Iterative loop for time
   - Solve the solid equations for new time.
   - Solve the gas equations to yield updated distributions of the solution variables with same values at $x = 0$ in step 3, except:

$$C_4(0) = \begin{cases} 0, & \text{if } 0 \le t \le t_0 \\ \dfrac{\delta}{v_{g_0}}, & \text{if } t > t_0 \end{cases}$$

$$C_6(0) = \begin{cases} \dfrac{0.79u_{0_{ol}}}{v_{g_0}}, & \text{if } 0 \le t < t_{cl} \\ \dfrac{0.79u_0(t+dt)}{v_{g_0}}, & \text{if } t \ge t_{cl} \end{cases}$$

$$C_7(0) = \begin{cases} \dfrac{0.21u_{0_{ol}}}{v_{g_0}}, & \text{if } 0 \le t < t_{cl} \\ \dfrac{0.21u_0(t+dt)}{v_{g_0}}, & \text{if } t \ge t_{cl} \end{cases}$$

5. Update time: $t^{n+1} = t^n + dt$
6. Stop if $t = t_{end}$, else go to step 4

However, the main objective of Table I is to show that how the control input interacts with the system.

The UCG system is operated in open loop for $0 \le t < t_{cl}$ with the input $u_{0_{ol}}$, and for $t \ge t_{cl}$ the operation is closed loop with the flow rate u_0. Actually the controller is brought in to the loop after the transients of the ignition phase are settled down.

The differential equation for the control input: $\dot{u} = -\kappa \operatorname{sign}(s)$ (Sec VI) is numerically solved using the forward Euler's mehtod [31] with $u(t_{cl}) = u_{ol}$.

$$u(t+dt) = -\kappa \operatorname{sign}\{s(t)\}dt + u(t) \tag{36}$$

where dt is the sampling time for the numerical solution.

The air flowrate u_0 at $x = 0$ is given by the following equation:

$$u_0(t+dt) = \frac{1}{\mathfrak{C}}\left[\mathfrak{D}u(t) - \mathfrak{E}u(t+dt) - \mathfrak{F}u_0(t) - \mathfrak{G}u_0(t-dt)\right] \tag{37}$$

$where,$

$$\mathfrak{C} = \frac{\tau_{d_a}\tau_a + \tau_{d_a}dt + 2\tau_a dt}{dt^2}$$

$$\mathfrak{D} = \frac{2dt^2 - 2\tau_a dt - \tau_{d_a}dt - 2\tau_{d_a}\tau_a}{dt^2}$$

$$\mathfrak{E} = \frac{\tau_{d_a}\tau_a}{dt^2}$$

$$\mathfrak{F} = \frac{2dt + \tau_{d_a}}{dt}$$

$$\mathfrak{G} = \frac{\tau_{d_a}}{dt}$$

The air flowrate u_0 determines the concentration of the O_2 and N_2 at $x = 0$ required to obtain the desired composition of the product gases. One part of u_0 directly affects the output as the inert gas N_2 does not participate in any chemical reaction and the other part influences the output through the UCG reactor model.

The output y is calculated by Eq. (48) and y_m in Fig. 1 is computed as:

$$y_m(t+dt) = \frac{1}{\mathfrak{H}}\left[\mathfrak{I}y(t) - \mathfrak{J}y(t+dt) - \mathfrak{K}y_m(t) - \mathfrak{L}y_m(t-dt)\right] \tag{38}$$

where $\mathfrak{H} = \mathfrak{C}(\tau_a = \tau_g, \tau_{d_a} = \tau_{d_g})$, $\mathfrak{I} = \mathfrak{D}(\tau_a = \tau_g, \tau_{d_a} = \tau_{d_g})$, $\mathfrak{J} = \mathfrak{E}(\tau_a = \tau_g, \tau_{d_a} = \tau_{d_g})$, $\mathfrak{K} = \mathfrak{F}(\tau_{d_a} = \tau_{d_g})$ and $\mathfrak{L} = \mathfrak{G}(\tau_{d_a} = \tau_{d_g})$

VIII. SIMULATION RESULTS

This section presents some simulation results for the closed loop system, in order to demonstrate the performance and robustness of the SMC technique. For simulations $t_{cl} = 1$ hr, $\tau_a = \tau_g = \tau_{d_a} = \tau_{d_g} = dt = 10$ s and the controller gain $\kappa = 2 \times 10^{-8}$.

The control effort in Fig. 4 drags y to y_r (Fig. 5). A critical amount of steam is required for the process of UCG to exist, otherwise the starvation or flooding of the UCG cavity can occur. Steam is responsible for the steam gasification reaction which produces CO and H_2. The steam participating in the gasification reaction is produced by the water influx from the surrounding aquifers. The amount of intruding water can be controlled by changing the operating pressure of the UCG reactor, but still there is an uncertainty in the actual amount of steam present in the reactor, because its measurement is not available. However, there is always an upper limit to the amount of steam available for the reactor, otherwise the flooding of the cavity occurs and extinguishes the burning of coal. The profile of δ used for evaluating the robustness of the SMC algorithm is shown in the Fig. 6. Despite the variation in δ the controller successfully keeps the output at its desired level. The increase in δ increases the production of syngas and hence y. The controller reacts to the situation by increasing u which provides more O_2 for char oxidation

reaction and results in higher concentration of CO_2, which decreases y by reducing the molar fractions of CO and H_2. Moreover, increasing u produces more moles of N_2 which directly decreases y. Similarly when δ decreases, the controller also reduces the moles of air entering the reactor to increase y.

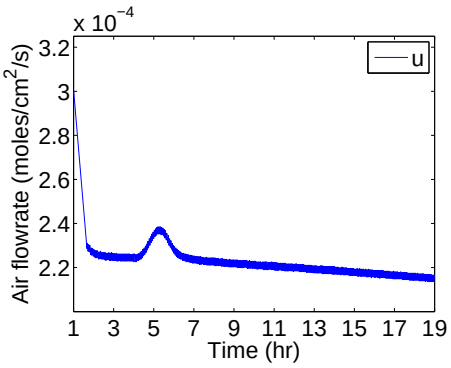

Fig. 4. Control effort with time

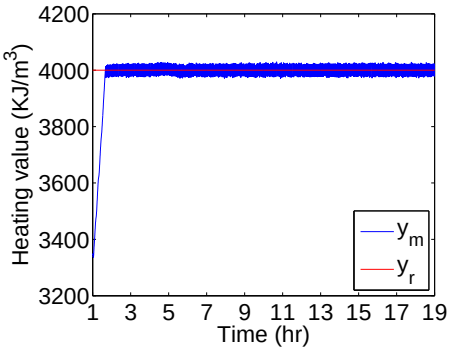

Fig. 5. Output of the UCG process with time

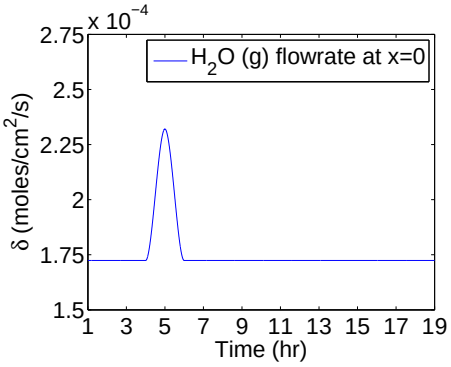

Fig. 6. Disturbance with time

The sliding variable s is shown in Fig. 7. In reaching phase: $s \neq 0$, the controller drags y to the sliding manifold in the presence of δ and modeling uncertainties. While the design of s keeps $y = y_r$ during the sliding motion: $s = 0$. The chattering phenomenon can also be seen in the zoomed view of Fig. 7, which is caused by finite sampling frequency of discretization: $f_s = 1/dt = 0.1$ hz, ignoring the dynamics of actuator and sensor, and by using a simplified UCG model during control design.

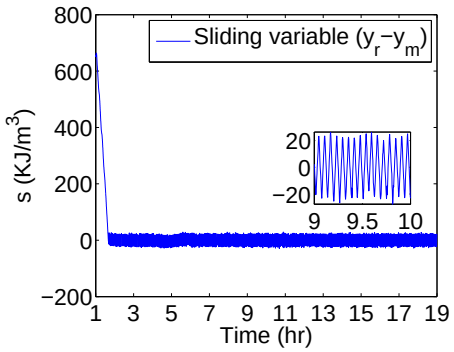

Fig. 7. Sliding variable with time

The solutions of the states of the UCG process are shown in Figs. 8, 9 and 10. The results are shown for 19 hrs and 400 cm, because during this time the coal bed is approximately consumed up to 350 cm.

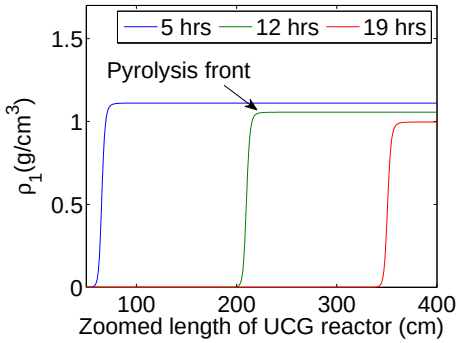

Fig. 8. Coal density distributions with length at different simulation times

Fig. 8 shows that the magnitude of the coal density distribution is decreasing with time, which justifies the solution for the mass balance of coal in Eq. (19). It can also be noticed that the distribution of coal density is pushed towards $x = L$ with time.

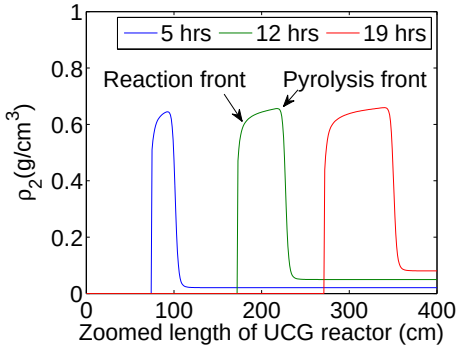

Fig. 9. Char density distributions with length at different simulation times

The magnitude of the ρ_2 distribution is increasing with time (Fig. 9) due to the coal pyrolysis reaction, but this increase

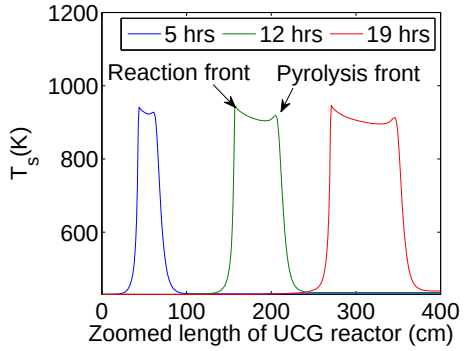

Fig. 10. Solid temperature distributions with length at different simulation times

lessens as ρ_1 decreases. It can also be observed that the width of the reaction zone Ω is also widening with time. The char density is consumed by R_2 and R_3 near the reaction front.

Fig. 10 shows that the T_s distributions have higher values in Ω. All the chemical reactions occur within this region, beyond this region the temperature is not high enough to support any chemical reaction. A high value of temperature is maintained within the reaction zone by the exothermic nature of coal pyrolysis and char oxidation reaction. Therefore, when all of the coal and char is consumed then there is no more fuel to be burnt, and the temperature will attain its lowest possible value determined by the respective boundary conditions.

The boundedness of the zero dynamics proved in Section VI-C can also be verified from the results in Figs. 8, 9 and 10.

IX. Conclusion

The SMC successfully maintains the desired heating value of the product gas mixture. The gain of the SMC is found by knowing the bounds of the auxiliary functions of the process variables. However, this methodology is applicable if in addition to tracking, the problem of stability is also solved. In our case it should be shown that so called zero dynamics are governed by a set of PDEs. For the mass balance equations, solutions were found analytically and a Lyapunov functional was found to demonstrate stability of the heat equation. The selected value of the controller gain also compensates for the input disturbance and the modeling approximations made for analytical control design. The simulation results show the success of the SMC algorithm.

The implementation of the designed SMC on the actual UCG site will further validate its effectiveness.

Appendix A
One Dimensional Packed Bed Model of Underground Coal Gasification

The actual model of UCG [25] is comprised of following equations.

A. Solid equations

These equations are based on the laws of conservation of mass and energy for coal and char.

$$\frac{\partial}{\partial t}\rho_i = M_i \sum_{j=1}^{6} a_{s_{ij}} R_j \tag{39}$$

$$where,$$

$$\rho_i\left(0,x\right) = \rho_{i_0}(x), \quad 0 \le x \le L$$

$$\frac{\partial T_s}{\partial t} = \frac{\frac{\partial}{\partial x}\left[(1-\phi)k\frac{\partial T_s}{\partial x}\right] + h(T-T_s) - H_s}{C_s} \tag{40}$$

$$where,$$

$$T_s\left(0,x\right) = T_{s_0}(x), \quad 0 \le x \le L$$

$$\frac{\partial T_s}{\partial x}\left(t,0\right) = \frac{\partial T_s}{\partial x}\left(t,L\right) = 0, \quad t \ge 0$$

where C_s is the total solid phase heat capacity (cal/K/cm^3) and H_s the solid phase heat source (cal/s/cm^3).

B. Gas equations

The gas phase equations are ordinary differential equations (ODEs) in x.

$$\frac{dC_i}{dx} = \frac{1}{v_g}\left(-C_i\frac{dv_g}{dx} + \sum_{j=1}^{3} a_{ij}R_j\right) \tag{41}$$

$$\frac{dT}{dx} = -\frac{h}{v_g C_g}\left(T - T_s\right) \tag{42}$$

$$\frac{dP}{dx} = -\frac{v_g \mu}{2K} \tag{43}$$

$$\frac{dv_g}{dx} = -\frac{v_g}{P}\frac{dP}{dx} + \frac{u_g}{T}\frac{dT}{dx} + \frac{RT}{P}\sum_{i=1}^{8}\sum_{j=1}^{3} a_{ij}R_j \tag{44}$$

where C_i is the concentration (mol/cm^3) of gas i with $i = 1 \to 8$ represents CO, CO_2, H_2, H_2O (g), CH_4, N_2, O_2 and tar, K is the gas permeability coefficient (cm^2), μ is the viscosity (Pa s) and R is the universal gas constant (cm^{3}Pa/mol/K).

C. Chemical kinetics

A set of six chemical reactions is considered in [25], but for the simplified model in Section III-A only three important reactions are considered, which include coal pyrolysis, char oxidation and steam gasification [25].

CH_aO_b and $CH_{\bar{a}}O_{\bar{b}}$ are the empirical formulas for the coal and char respectively with a, b, $\bar{a}$ and $\bar{b}$ are determined by the coal and char ultimate analysis.

The equations for the rates of the reaction are as follows:

1) Coal pyrolysis:

$$R_1 = 5\frac{\rho_1}{M_1}\exp\left(\frac{-6039}{T_s}\right) \tag{45}$$

TABLE II
CHEMICAL REACTIONS CONSIDERED IN THE MODEL

Sr	Chemical equations
1.	**Pyrolysis** $CH_aO_b \rightarrow \lvert a_{s_{2,1}}\rvert CH_{\bar{a}}O_{\bar{b}} + \lvert a_{1,1}\rvert CO + \lvert a_{2,1}\rvert CO_2 + a_{3,1}H_2 + \lvert a_{4,1}\rvert H_2O + \lvert a_{5,1}\rvert CH_4 + \lvert a_{8,1}\rvert C_9H_c$
2.	**Char Oxidation** $CH_{\bar{a}}O_{\bar{b}} + \lvert a_{7,2}\rvert O_2 \rightarrow \lvert a_{2,2}\rvert CO_2 + \lvert a_{4,2}\rvert H_2O$
3.	**Steam gasification** $CH_{\bar{a}}O_{\bar{b}} + \lvert a_{4,3}\rvert H_2O \rightleftharpoons \lvert a_{1,3}\rvert CO + \lvert a_{3,3}\rvert H_2$

2) Char oxidation:

$$R_2 = \frac{1}{\frac{1}{R_{c_2}} + \frac{1}{k_y m_7}} \tag{46}$$
$$R_{c_2} = \frac{9.55 \times 10^8 \rho_2 m_7 P \exp\left(\frac{-22142}{\tilde{T}}\right)\tilde{T}^{-0.5}}{M_2}$$
$$\tilde{T} = \beta T_s + (1-\beta)\,T$$

where m_7 is the mole fraction of O_2 and $\beta = 1$

3) Steam gasification:

$$R_3 = \begin{cases} \frac{1}{\frac{1}{R_{c_3}} + \frac{1}{k_y m_4}}, & \text{if } m_4 - \left(\frac{m_1 y_3}{K_{E_3}}\right) > 0 \\ \frac{1}{\frac{1}{R_{c_3}} - \frac{1}{k_y y_1}}, & \text{if } m_4 - \left(\frac{m_1 m_3}{K_{E_3}}\right) < 0 \end{cases} \tag{47}$$
$$R_{c_3} = \frac{{R_{c_3}}^+}{m_4}\left(m_4 - \frac{m_1 m_3}{K_{E_3}}\right)$$
$${R_{c_3}}^+ = \frac{\rho_2 m_4^2 P^2 \exp\left(5.052 - \frac{12908}{\tilde{T}}\right)}{M_2\left[m_4 P + \exp\left(-22.216 + \frac{24880}{\tilde{T}}\right)\right]^2}$$

where m_1,m_3 and m_4 are molar fractions of CO, H_2 and H_2O respectively, and K_{E_3} is equilibrium constant for steam gasification reaction.

D. Model simplification

In order to make the control design analytically possible, following assumptions are considered in the actual model.

- It is assumed that the pressure of the gas mixture is constant along the length of the reactor. If a well linked channel is established between the injection and production wells then the gas pressure does not drop significantly through the UCG channel [24].
- Only the rate of forward reaction is considered for steam gasification in Eq. (47). The concentration of steam does not vary much along the reactor, therefore it is assumed that it stays equal to its intial value $\frac{\delta}{v_{g_0}}$. This assumption further simplifies R_3.
- It is also assumed that the total concentration of the gases near the reaction front(location along the length of the reactor where the injected air reacts with the hot char [25]) is the sum of the concentrations of H_2O (g), N_2 and O_2. Actually the sum of the concentrations of these three gases dominate the total concentration at the reaction front. As R_2 and R_3 are only significant near the reaction front so this approximation reduces the complexity of Eqs. (46) and (47).
- The parameters like heat transfer coefficient h, mass transfer coefficient k_y, gas phase velocity v_g, total gas phase heat capacity C_g and the thermal conductivity of the coal and char k are considered constant to simplify control design.

APPENDIX B
DERIVATION OF THE HEATING VALUE

After the removal of H_2O (g) from the product gases, the gas mixture is sent to the gas analyzer which initially measures the molar fraction of the gases and then calculates the heating value [24], [25].

$$y = H_1 m_1(L) + H_3 m_3(L) + H_5 m_5(L) + H_8 m_8(L) \tag{48}$$
$$m_i = 100 \times \frac{C_i(L)}{\tilde{C_T}(L)}$$
$$\tilde{C_T}(L) = \sum_{i=1, i\neq 4}^{8} C_i(L)$$

where m_i is the molar fraction of gas i, and $\tilde{C_T}$ is the sum of the concentration of all the gases except H_2O (g).

The Eq. (41) is solved to yield $C_i(L)$ by assuming v_g to be constant. The solution for CO, CO_2, H_2, CH_4 and tar at $x = L$ with $C_i(0) = 0$ is:

$$C_i(L) = \frac{1}{v_g}\sum_{j=1}^{3} a_{i,j}\int_0^L R_j dx \tag{49}$$

The solution for $C_7(L)$, with $C_7(0) = 0.21\frac{u}{v_g}$ is:

$$\frac{dC_7}{dx} = -\frac{|a_{7,2}|}{v_g}R_2$$
$$C_7(L) = 0.21\frac{u}{v_g}\exp\left(-\frac{|a_{7,2}|}{u+\delta}\int_0^L CR_2\right) \tag{50}$$

N_2 is an inert gas and it does not participate in any chemical reaction, therefore $C_6(L) = C_6(0) = 0.79\frac{u}{v_g}$.

Almost all of the O_2 is consumed by the char oxidation reaction at the reaction front [25], so it is assumed that $C_7(L) = 0$. The expression for $C_7(L)$ also supports this argument. Therefore, by substituting the concentration of the gases in Eq. (48) the Eq. (9) can be obtained.

ACKNOWLEDGMENT

The authors would like to acknowledge control and signal processing research (CASPR) group at Muhammad Ali Jinnah University, electrical and computer engineering department of the Ohio State University, electrical and computer engineering department of COMSATS institute of information technology, UCG project Thar, national ICT R&D funds and higher education commission (HEC) of Pakistan.

REFERENCES

[1] A. W. Bhutto, A. A. Bazmi, and G. Zahedi, "Underground coal gasification: From fundamentals to applications," *Progress in Energy and Combustion Science*, vol. 39, no. 1, pp. 189 – 214, 2013.

[2] A. Khadse, M. Qayyumi, S. Mahajani, and P. Aghalayam, "Underground coal gasification: A new clean coal utilization technique for India," *Energy*, vol. 32, no. 11, pp. 2061 – 2071, 2007.

[3] D. W. Gregg and T. F. Edgar, "Underground coal gasification," *AIChE Journal*, vol. 24, no. 5, pp. 753–781, 1978.

[4] A. Khadse, M. Qayyumi, and S. Mahajani, "Reactor model for the underground coal gasification UCG channel," *International Journal of Chemical Reactor Engineering*, vol. 4, no. 1, 2006.

[5] G. M. P. Perkins, *Mathematical Modelling of Underground Coal Gasification*. PhD thesis, The University of New South Wales, 2005.

[6] C. Magnani and S. Farouq Ali, "Mathematical-modeling of stream method of underground coal gasification," *Society of Petroleum Engineers Journal*, vol. 15, pp. 425 – 436, 1975.

[7] C. Magnani and S. Farouq Ali, "A two-dimensional mathematical model of the underground coal gasification process," in *Fall Meeting of the Society of Petroleum Engineers of AIME*, 1975.

[8] C. B. Thorsness and R. B. Rozsa, "Insitu coal-gasification: Model calculations and laboratory experiments," *Society of Petroleum Engineers Journal*, vol. 18, pp. 105–116, 1978.

[9] E. N. J. Beizen, *Modeling Underground Coal Gasification*. PhD thesis, Delft University of Technology, Delft, Netherlands, 1996.

[10] L. Yang, "Model and calculation of dry distillation gas movement in the process of underground coal gasification," *Numerical Heat Transfer, Part B: Fundamentals*, vol. 43, no. 6, pp. 587–604, 2003.

[11] G. Perkins and V. Sahajwalla, "A mathematical model for the chemical reaction of a semi-infinite block of coal in underground coal gasification," *Energy & Fuels*, vol. 19, no. 4, pp. 1679–1692, 2005.

[12] G. Perkins and V. Sahajwalla, "Modelling of heat and mass transport phenomena and chemical reaction in underground coal gasification," *Chemical Engineering Research and Design*, vol. 85, no. 3, pp. 329 – 343, 2007.

[13] K.-H. Wolf and H. Bruining, "Modelling the interaction between underground coal fires and their roof rocks," *Fuel*, vol. 86, no. 1718, pp. 2761 – 2777, 2007.

[14] G. Perkins and V. Sahajwalla, "Steady-state model for estimating gas production from underground coal gasification," *Energy & Fuels*, vol. 22, no. 6, pp. 3902–3914, 2008.

[15] M. Seifi, J. Abedi, and Z. Chen, "Application of porous medium approach to simulate UCG process," *Fuel*, vol. 116, no. 0, pp. 191 – 200, 2014.

[16] K. Kostúr and J. Kačúr, "The monitoring and control of underground coal gasification in laboratory conditions," *Acta Montanistica Slovaca*, vol. 13, no. 1, pp. 111–117, 2008.

[17] K. Kostur and J. Kacur, "Development of control and monitoring system of UCG by promotic," in *2011 12th International Carpathian Control Conference (ICCC)*, pp. 215 –219, may 2011.

[18] K. J. Aström and T. Hägglund, *PID Controllers: Theory, Design, and Tuning*. Instrument Society of America, Research Triangle Park, NC, 2 ed., 1995.

[19] V. Utkin, "Control of distributed-parameter plants," in *Sliding Modes in Control and Optimization*, Communications and Control Engineering Series, pp. 169–188, Springer Berlin Heidelberg, 1992.

[20] K. Morris, "Control of systems governed by partial differential equations," in *Electrical Engineering Handbook*, ch. 67, pp. 1–37, CRC Press, 2010.

[21] I. U. Vadim, "Survey paper variable structure systems with sliding modes," *IEEE Transactions on Automatic control*, vol. 22, no. 2, pp. 212–222, 1977.

[22] K. Young, V. Utkin, and U. Ozguner, "A control engineer's guide to sliding mode control," *Control Systems Technology, IEEE Transactions on*, vol. 7, pp. 328–342, May 1999.

[23] A. Arshad, A. Bhatti, R. Samar, Q. Ahmed, and E. Aamir, "Model development of ucg and calorific value maintenance via sliding mode control," in *2012 International Conference on Emerging Technologies (ICET)*, pp. 1–6, 2012.

[24] A. A. Uppal, A. I. Bhatti, E. Aamer, R. Samar, and S. A. Khan, "Optimization and control of one dimensional packed bed model of underground coal gasification," *Journal of Process Control*, vol. 35, pp. 11 – 20, 2015.

[25] A. A. Uppal, A. I. Bhatti, E. Aamir, R. Samar, and S. A. Khan, "Control oriented modeling and optimization of one dimensional packed bed model of underground coal gasification," *Journal of Process Control*, vol. 24, no. 1, pp. 269–277, 2014.

[26] J. E. Slotine and W. Li, *Applied Nonlinear Control*. Englewood Cliffs, NJ: Prentice-Hall, 1991.

[27] D. U. Olness and L. L. N. Laboratory, *The Podmoskovnaya underground coal gasification station*. Livermore, Calif. : Lawrence Livermore Laboratory, University of California, 1981.

[28] A. Fossard and T. Floquet, "An overview of classical sliding mode control," in *Sliding Mode Control in Engineering* (J. P. Barbot and W. Perruquetti, eds.), Control Engineering, New York, NY, USA: Marcel Dekker, Inc., 2002.

[29] V. Utkin, "Sliding mode control in discrete-time and difference systems," in *Variable Structure and Lyapunov Control* (A. Zinober, ed.), vol. 193 of *Lecture Notes in Control and Information Sciences*, pp. 87–107, Springer Berlin Heidelberg, 1994.

[30] G. H. Golub and C. F. V. Loan, "Functions and matrices," in *Matrix Computations*, pp. 555–578, The Johns Hopkins University Press, Baltimore and London, 3 ed., 1996.

[31] W. Y. Yang, W. Cao, T.-S. Chung, and J. Morris, "Applied numerical methods using matlab," *America*, vol. 47, p. 509, 2005.